Available online at www.sciencedirect.com
ScienceDirect
Trans. Nonferrous Met. Soc. China 27(2017) 901−907
Transactions of Nonferrous Metals Society of China
www.tnmsc.cn

Leaching of iron concentrate separated from kiln slag in zinc hydrometallurgy with hydrochloric acid and its mechanism

Hong-jun WANG[1,2], Zhi-yong LIU[1], Zhi-hong LIU[1], Yu-hu LI[1], Si-wei LI[1], Wen-Hai ZHANG[1,2], Qi-hou LI[1]

1. School of Metallurgy and Environment, Central South University, Changsha 410083, China;
2. Institute of Metallurgy, China Nerin Engineering Co., Ltd., Nanchang 330031, China

Received 25 September 2016; accepted 23 February 2017

Abstract: It is taken as a novel prospective process to treat iron concentrate from hydrometallurgical zinc kiln slag for comprehensive utilization of valuable metals by a hydrochloric acid leaching-spray pyrolysis method. The leaching mechanism of different valuable metals was studied. The results revealed that the leaching rates of Ag, Pb, Cu, Fe, As and Zn were 99.91%, 99.25%, 95.12%, 90.15%, 87.58% and 58.15%, respectively with 6 mol/L HCl and L/S ratio of 10:1 at 60 °C for 120 min. The action of SiO_2 in leaching solution was also studied. The results showed that the precipitation and settlement of SiO_2(amorphous) adsorbed part of metal ions in solution, which greatly inhibited the leaching of Cu, Fe, As and Zn, so it is crucial to control the precipitation of amorphous SiO_2.

Key words: kiln slag; iron concentrate; hydrochloric acid leaching; amorphous silica

1 Introduction

Zinc is primarily produced from sulfide concentrates by using roast−leach−electrowinning process in the world. A rock-ribbed problem of this process is the generation of large amounts of unmanageable zinc leaching residues containing valuable metals and toxic elements, such as lead, copper, silver and arsenic [1−3]. If the residues are not effectively treated, not only the environment will be seriously polluted, but also the resources will be wasted [4−6]. Zinc leaching residues can be treated by pyrometallurgical or hydrometallurgical processes. The hydrometallurgical-process commonly involves flotation and leaching [7], sulphation roasting-leaching [8−10], chloride leaching [11], hot acid leaching-jarosite (goethite or hematite) process, etc, [12−14]. Due to high reagent consumption, severe corrosion of equipment, a large amount of iron precipitation residues and unstable recovery rate, disposal of zinc residues is now mainly focused on pyrometallurgical processes, such as waelz kiln volatilization [1,15,16], fuming [17], top blown smelting [18,19], QSL and Kivcet [20], etc. The mostly widely used process in China is waelz kiln volatilization due to its low investment and operation cost [21].

Most of Zn, Pb and Cd are reduced and volatized from zinc residues to zinc oxide dust in waelz kiln process, Cu, Ag, Fe and part of carbon, Zn, Pb, and As are left in the kiln slag. In recent years, many domestic enterprises conducted comprehensive utilization of the kiln slag by gravity and magnetic separation, in which coke powder, iron concentrate and tailings are obtained. Coke powder is returned to the production system as fuel, iron concentrate is the raw material for iron making and tail slag is used for making cement [22]. This process has been applied to industrial production and has achieved certain economic benefits. But the problem is that iron concentrate can only be used with a small amount in iron making because of its high contents of S, Zn and As. Meanwhile, the valuable metals have not been effectively recycled, such as Cu，Ag and In [23,24].

2 Experimental

2.1 Materials and apparatus

The iron concentrate used in the present study was obtained from Zinc Smelting Company of Shangluo in

Foundation item: Project (51404307) supported by the National Natural Science Foundation of China; Project (2014CB643400) supported by the National Basic Research Program of China
Corresponding author: Zhi-yong LIU; Tel: +86-731-88830478; E-mail: csuliuzhiyong@163.com
DOI: 10.1016/S1003-6326(17)60104-3

Shanxi Province, China. The iron concentrate was dried, ground. Particle analysis found that the sizes of >90% particles were smaller than 109 μm. The ore was analyzed via a chemical method and phase-examined by using powder X-ray diffraction (XRD). The scanning speed was 10 (°)/min.

Chemical leaching experiments were conducted in batches with 100 g/L solids in a 1000 mL solution in a glass flask (total volume, 2000 mL) immersed in a thermostatic water bath agitated by a mechanical agitator. The reaction between the iron concentrate ore and hydrochloric acid was at (30±0.1) °C and the mixture was agitated at a rate of 350 r/min. The leach solutions were prepared using analytical reagent hydrochloric acid and distilled water. Hydrochloric acid concentration was 6 mol/L, and the pH value of the final solution was around 0.1 in the study. At selected time intervals, the sample was separated via centrifugation, washed three times with distilled water, and then dried in an oven at 60 °C.

2.2 Sample characterization

The iron concentrate was characterized via powder XRD analysis using a Japan Rigaku Model TTRIII+ 40 kV/250 mA with Cu K_α radiation. The different diffraction peaks were analyzed for various phases and compared with the ASTM standard.

IR spectra were obtained using an America Nicolet IS 10 spectrometer with a smart endurance single-bounce diamond ATR cell. The samples were prepared using the KBr pellet method. The spectra over the range from 4000 to 400 cm^{-1} were obtained at a resolution of 4 cm^{-1} and a mirror velocity of 0.6329 cm/s. The spectra were coadded to improve the signal-to-noise ratio.

Both crude and leach residues were also analyzed via SEM. The samples were mounted on a copper stub, and the analysis was performed using a Japan Jeol JSM−6360LV instrument equipped with a spectrometer for microanalysis based on an energy dispersive X-ray spectroscopy (EDS) system (EDX-GENESIS 60S, EDAX, USA) with an accelerating voltage of 0.5 kV to 30 kV.

The thermal analysis and mass loss were measured via thermogravimetric analysis (TGA) using a differential scanning calorimetry (DSC)-TGA SDT.Q600 instrument at a heating rate of 5 °C/min to reach the maximum temperature of 1000 °C in air atmosphere (100 cm^3/min).

3 Results and discussion

3.1 Characterizations of iron concentrate

The kiln slag iron concentrate sample was obtained from Shangluo Smelter, Shanxi Zinc Industry Co., Ltd., Shanxi Province, China. Table 1 shows that >90% particles were smaller than 109 μm.

Table 1 Particle size distribution of kiln slag iron concentrate sample

Particle size/μm	Content/%
<47	52.57
47−53	6.01
53−62	10.74
62−80	14.00
80−109	13.68
>109	3.00
Total	100

The chemical and iron-containing phase compositions of the sample are shown in Tables 2 and 3, respectively. The XRD pattern of the kiln slag iron concentrate sample, as presented in Fig. 1, shows only four main phases of Fe_3O_4, $CuFe_2O_4$, Fe_2O_3 and SiO_2 with no evidence of other phases, probably due to their less content or lower crystallinity. Figure 2 indicates that the sample was composed of aggregates of micron-sized particles with some massive and dense bulks present, which may be the agglomeration of semi molten kiln

Table 2 Chemical composition of kiln slag iron concentrate sample (mass fraction, %)

Fe	Zn	Cu	Pb	As	S	SiO_2	Al_2O_3	MnO	Ag*
56.4	2.51	2.51	0.99	0.49	4.75	2.31	1.85	1.28	265

* The mass fraction of Ag is in g/t.

Table 3 Composition of iron-containing phases in kiln slag iron concentrate sample (mass fraction, %)

FeS	$FeSO_4$	Fe	Fe_3O_4	Fe_2O_3	$FeSiO_3$
6.63	1.38	16.63	67.85	2.39	5.08

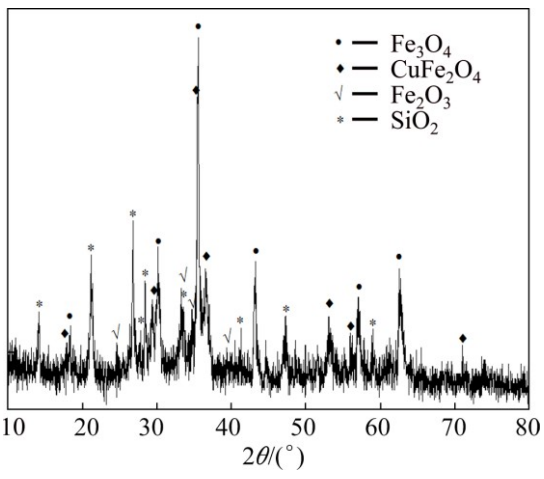

Fig. 1 XRD pattern of kiln slag iron concentrate sample

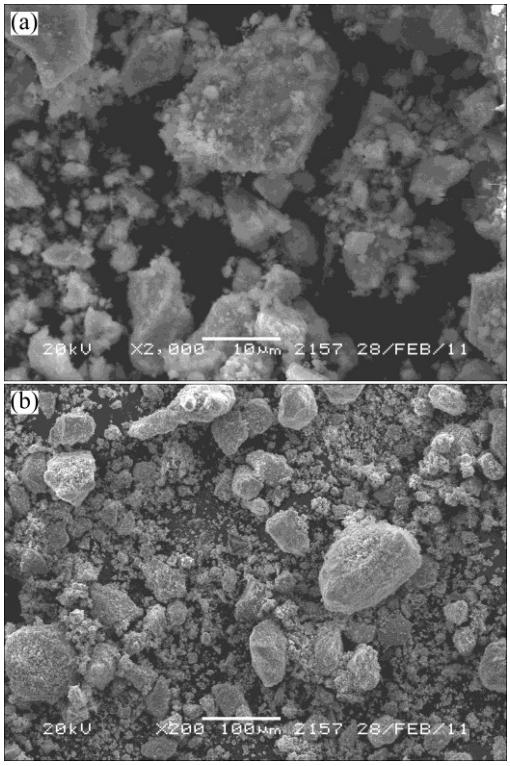

Fig. 2 SEM image of kiln slag iron concentrate sample

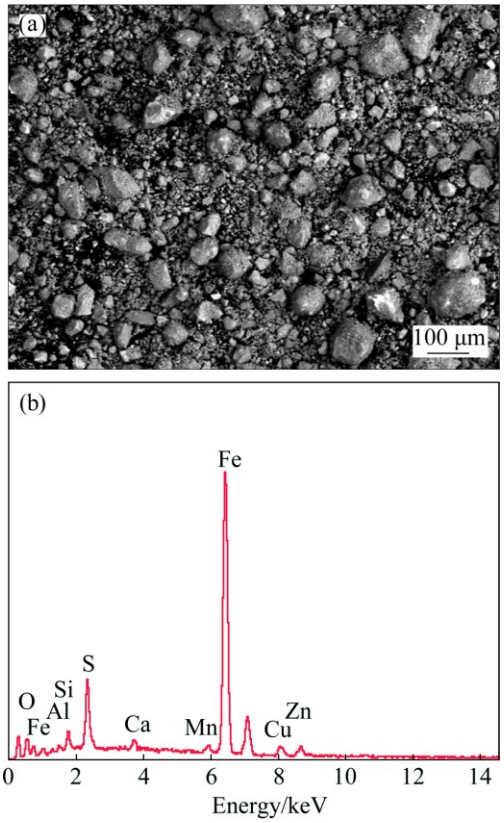

Fig. 3 BSE image (a) and corresponding EDS spectrum (b) of kiln slag iron concentrate sample

slag formed during high temperature reduction volatilization process. The EDS result of kiln slag iron concentrate, as shown in Fig. 3, was in accord with the chemical analysis.

3.2 Leaching mechanism of iron concentrate

The effect of time on leaching rate, as shown in Fig. 4, indicates that the leaching rates of lead, copper, iron, arsenic and zinc were not very high, which were 82.05%, 70.02%, 80.12%, 75.06% and 38.65% at 120 min, respectively, especially for zinc, which only increased from 36.56% at 30 min to 38.65% at 120 min. In addition, the leaching rate decreased slightly with the increase of time after 120 min. It can be inferred that some substance inhibited the leaching, and the longer the time, the greater the inhibition. However, there was no this kind of inhibition effect in the leaching process of silver for its low content in the sample.

When the optimal leaching conditions were determined to be 6 mol/L HCl with L/S ratio of 10:1 at 60 °C for 120 min. The results are shown in Table 4. Under these conditions, the leaching rates of silver, lead, copper, iron, arsenic and zinc were 99.91%, 99.25%, 95.12%, 90.15%, 87.58% and 58.15%, respectively.

The EDS analysis result of the leaching residue is shown in Fig. 5. The characteristic peaks of S, Zn, Cl, Fe and Si are obvious, where the Cl came from remaining $FeCl_2$.

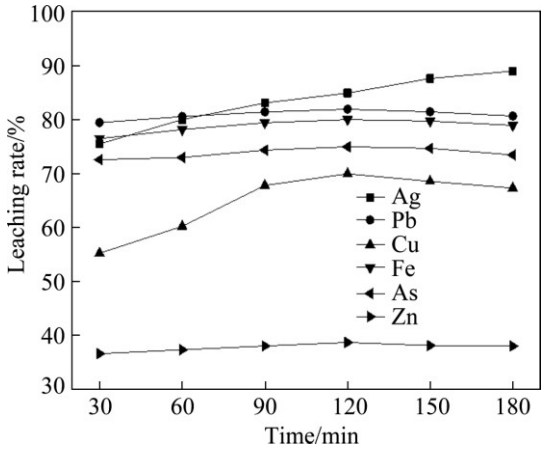

Fig. 4 Effect of leaching time on leaching rate (6 mol/L HCl and L/S of 10:1 at 30 °C)

Table 4 Leaching rate of elements (%)

Fe	Ag	Cu	Pb	As	Zn
90.15	99.91	95.12	99.25	87.58	58.15

Figure 6 indicates the diffraction lines of FeS, ZnS and SiO_2 with no lines associated with silver, lead and copper. It can be inferred that FeS and ZnS have not been fully leached out from iron concentrates, which is the reason why the leaching rate of iron remains at around 90%, and the leaching rate of Zn is as low as about 60%.

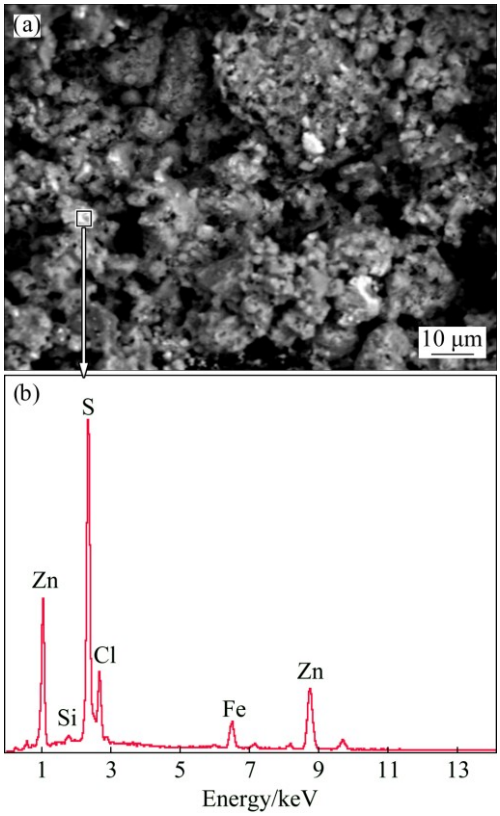

Fig. 5 BSE image (a) and corresponding EDS spectrum (b) of leaching slag

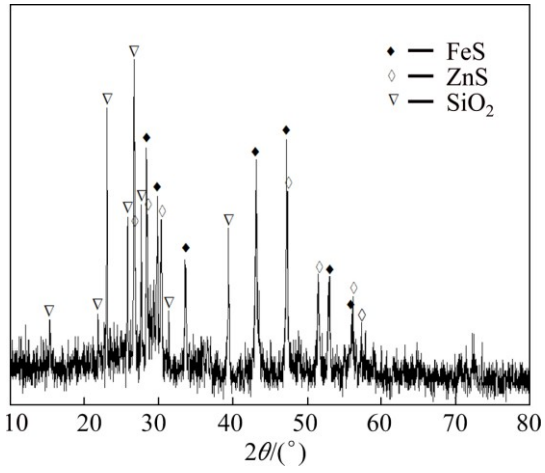

Fig. 6 XRD pattern of leaching slag

The thermodynamics in iron and zinc hydrometallurgical process was studied using a chemical equilibrium modeling code (GEMS) to predict the iron and zinc solubility and construct the species distribution and predominance diagrams for the Fe−Cl−S−H_2O and Zn−Cl−S−H_2O system, as shown in Figs. 7 and 8. The distribution and predominance diagrams show that FeS and ZnS were stable, and can hardly be dissolved, which was in accord with the diffraction results of XRD pattern.

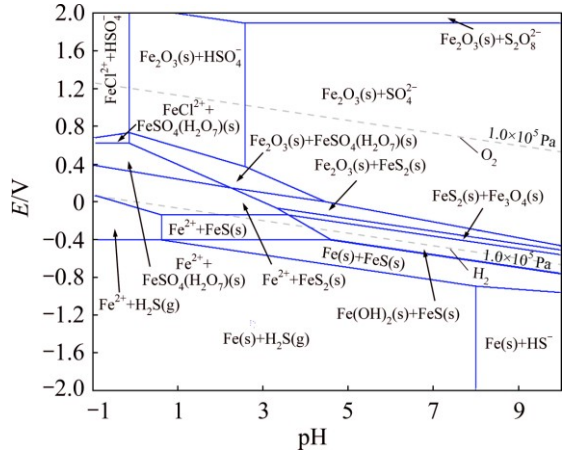

Fig. 7 *E*−pH diagram of Fe−Cl−S−H_2O system (333.15 K, $c(Cl^-)$=6 mol/L, $c(Fe^{n+})$=1 mol/L)

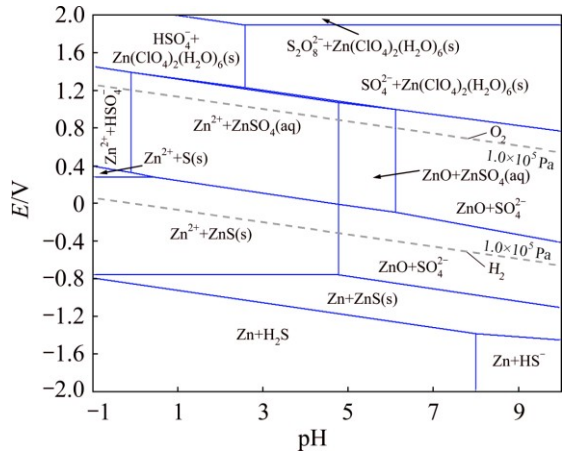

Fig. 8 *E*−pH diagram of Zn−Cl−S−H_2O system (333.15 K, $c(Cl^-)$=6 mol/L, $c(Zn^{n+})$=1 mol/L)

4 Action of silica in leaching solution

The silica concentration in the solution was kept at approximately 0.3 g/L because Si will precipitate into silicic acid, amorphous silicon dioxide, hydrated silicon dioxide, and other forms. Transparent gelatinous substance appeared when the leaching solution of optimum condition was kept still in beaker for 10 h, which increased and turned into white gradually. The composition of the gelatinous substance listed in Table 5 shows that the gelatinous substance contains a few impurities.

Table 5 X-ray fluorescence result of precipitation (mass fraction, %)

Al_2O_3	SiO_2	Fe_2O_3	CuO	ZnO	SO_3	As_2O_3
0.060	98.970	0.231	0.010	0.018	0.467	0.0479

The XRD pattern of the gelatinous substance is presented in Fig. 9. New low-intensity peaks corresponding to the amorphous material appear. The

result shows that the spectrum of the amorphous material is congruent with that of standard card PDF No.45−0423, which indicates its nature as hydrogen silica hydrate. When the diffraction angle is at around 25°, the XRD peaks are similar to those of the synthesized amorphous SiO_2 powder reported in a previous study [23]. As the leaching process progressed, the iron concentrate constantly dissolved, and amorphous SiO_2 or other materials with structure similar to that of amorphous SiO_2, such as hydrated silicon dioxide and hydrogen silica hydrate, are precipitated.

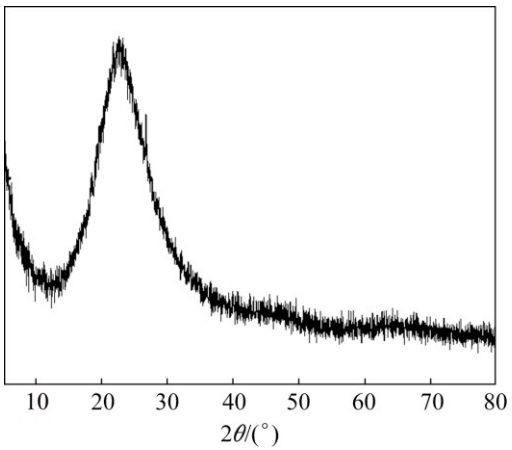

Fig. 9 XRD pattern of gelatinous substance

Figure 10 shows that the gelatinous substance and amorphous silicon dioxide have the same IR spectra. The characteristic bands appear at 3440.53, 1640.71, 1385.66, 1110.85, 969.09, 797.93 and 468.63 cm^{-1}. FARMER [25] and WEN [26] have shown that the IR spectra of quartz, tridymite, cristobalite, silica glass, and opal in the range of 1250−400 cm^{-1} are similar. Aside from the four-coordinated typical characteristic bands of SiO_2 at 1094, 800, and 470 cm^{-1}, the Si—O stretching vibration peak from the Si—OH groups of the newly precipitated silica also appears at 950 cm^{-1}. However, the Si—OH groups continue to polymerize and form Si—O—Si, and the characteristic bands disappear at 950 cm^{-1}.

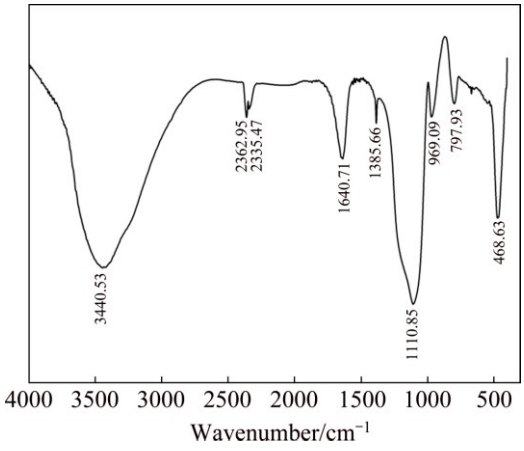

Fig. 10 Infrared (IR) spectra of gelatinous substance

The TGA−DSC results of the gelatinous substance are shown in Fig. 11. In the heat treatment process, the mass loss increases with the heat treatment temperature. When the temperature reaches 259.93 °C, the mass loss is 9.8%. This behavior may be due to the presence of crystal water in the leaching residue.

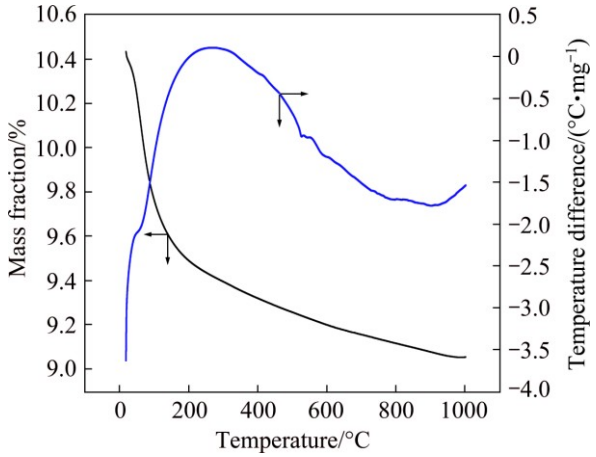

Fig. 11 TGA−DSC curves of gelatinous substance in air with temperature increase rate of 5 K/min

The FTIR, XRD and TGA−DSC results show that the aggregates and cross-linked spherical particles of the leaching residue are hydrated silicon dioxide. Therefore, it can be inferred that the silica gel was generated during the leaching process.

According to the FTIR, XRD and TGA−DSC analysis results, the leaching process can be divided into two stages: the first is iron silicate dissolution, and the second is silicic acid polymerization. During this process, the characteristic O—H structural band in water disappears at 3440.53 cm^{-1}, but the crystal water characteristic band at 1630 to 1640 cm^{-1} remains, indicating that the gelatinous substance contains crystal water. In the range of 1100−400 cm^{-1}, the characteristic band transforms into that of the new silica. The IR spectrum of the gelatinous substance is similar to that of the amorphous hydrated silicon dioxide, suggesting that $Si(OH)_4$ transforms into $SiO_2 \cdot nH_2O$ during the leaching process.

The dissolution equilibrium diagram of $SiO_{2(amorphous)}$, presented in Fig. 12, shows that the solubility of $SiO_{2(amorphous)}$ is very low and maintains constant when pH is lower than 9, which rises rapidly with the continuous increase of pH.

According to the dissolution equilibrium of silicate, the silicon species distribution diagrams in aqueous solution were drawn, which showed that almost all the silicon existed in combined single silicate acid molecular when the pH was lower than 7 [27−29]. The concentration of $H_2SiO_{3(aq)}$ continued to increase and reached saturation with the constant dissolution of

silicate in solution, then silicon precipitated as amorphous SiO_2. The results of Fig. 12 are consistent with those of DIETZEL [27]. The reaction is as follows:

$$H_2SiO_{3(aq)}=SiO_{2(amorphous)}+H_2O$$

$$K_s=[H_2SiO_{3(aq)}]=10^{-2.72}$$

The precipitated $SiO_{2(amorphous)}$ absorbed on the mineral surface did not react, which inhibited the leaching of other compounds and absorbed the metal ions dissolved. That was why the leaching rates of lead, arsenic, iron, copper and zinc declined with the time after 120 min. The precipitation of $SiO_{2(amorphous)}$ had little influence on the leaching of silver due to its low content in sample.

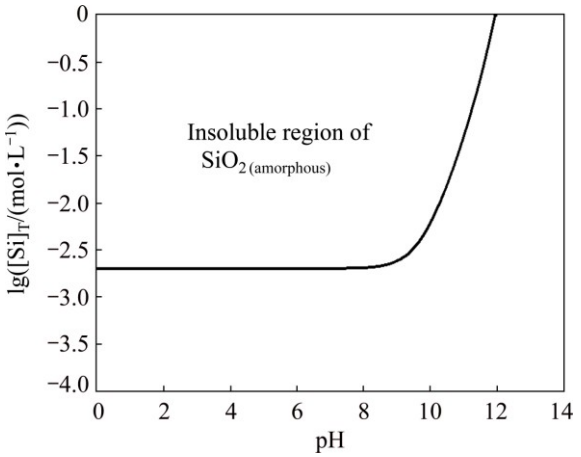

Fig. 12 lg[Si]$_T$−pH diagram of $SiO_{2(amorphous)}$

5 Conclusions

1) The iron concentrate contains 50%−60% of iron, together with some valuable nonferrous metals worth recovering, such as Ag, Cu, Pb and Zn, but its phase composition is quite complicated and most of the valuable metals are in forms of solid solutions or tiny particles of reticular structures, which makes the comprehensive recovery more difficult.

2) On the basis of thermodynamic analysis, the leaching experiments were carried out and the optimal condition was determined on the kiln slag iron concentrate. The leaching rates of Ag, Pb, Cu, Fe, As and Zn were 99.91%, 99.25%, 95.12%, 90.15%, 87.58% and 58.15%, respectively, with such optimal condition as 6 mol/L HCl and L/S ratio of 10:1 at 60 °C for 120 min.

3) Silicon dissolved in solution as $H_2SiO_{3(aq)}$, then precipitated as $SiO_{2(amorphous)}$ with the increase of time, which adsorbed part of metal ions in solution and inhibited the leaching, especially for Zn.

4) The leaching process can be divided into two stages: the first is iron silicate dissolution, and the second is silicic acid polymerization.

5) The main components of leaching residue were FeS, ZnS and SiO_2, which can be recycled to zinc roasting system.

References

[1] LIU Yang, TAN Jun, YIN Zhou-lan, LIU Chang-qing, CHEN Qi-yuan, ZHANG Ping-min, LIAO Zhou, WANG Xin-hao. Roasting pretreatment of iron-sinking slag and zinc leaching residue in zinc hydrometallurgy [J]. The Chinese Journal of Nonferrous Metals, 2016, 26(1): 212−222. (in Chinese)

[2] TURAN M D, ALTUNDOĞAN H S, TÜMEN F. Recovery of zinc and lead from zinc plant residue [J]. Hydrometallurgy, 2004, 75(1−4): 169−176.

[3] LIU Yang, TAN Jun, LIU Chang-qing, YIN Zhou-lan, CHEN Qi-yuan, ZHANG Ping-min, LIAO Zho. Thermodynamic analysis on iron-making process of zinc leaching residue by carbon reduction[J]. The Chinese Journal of Nonferrous Metals, 2015, 25(7): 1978−1986. (in Chinese)

[4] LI Mi, PENG Bing, CHAI Li-yuan, PENG Ning, YAN Huan, HOU Dong-ke. Recovery of iron from zinc leaching residue by selective reduction roasting with carbon [J]. Journal of Hazardous Materials, 2012, 237: 323−330.

[5] ÖZVERDI A, ERDEM M. Environmental risk assessment and stabilization/solidification of zinc extraction residue: I. Environmental risk assessment [J]. Hydrometallurgy, 2010, 100(3−4): 103−109.

[6] LI Yu-hu, LIU Zhi-hong, LI Qi-hou, ZHAO Zhong-wei, LIU Zhi-yong, ZENG Li. Removal of arsenic from Waelz zinc oxide using a mixed NaOH−Na_2S leach [J]. Hydrometallurgy, 2011, 108: 165−170.

[7] RASHCHI F, DASHTI A, ARABPOUR-YAZDI M, ABDIZADEH H. Anglesite flotation: A study for lead recovery from zinc leach residue [J]. Minerals Engineering, 2005, 18(2): 205−212.

[8] APARAJITH B, MOHANTY D B, GUPTA M L. Recovery of enriched lead–silver residue from silver-rich concentrate of hydrometallurgical zinc smelter [J]. Hydrometallurgy, 2010, 105(1): 127−133.

[9] WANG Rui-xiang, ZENG Jie, LI Jin-hui, TANG Mo-tang. Recovery of zinc and silver from zinc acid-leaching residue by sulphation roasting-water leaching of zinc and iron-silver chlorination leaching method [C]//2011 International Conference on Computer Science and Service System (CSSS). Nanjing, 2011: 576−580.

[10] WANG Y, ZHOU C. Hydrometallurgical process for recovery of cobalt from zinc plant residue [J]. Hydrometallurgy, 2002, 63(3): 225−234.

[11] TURAN M D, SAFARZADEH M S. Separation of zinc, cadmium and nickel from ZnO−CdO−NiO mixture through baking with ammonium chloride and leaching [J]. Hydrometallurgy, 2012, 119: 1−7.

[12] LOAN M, NEWMAN O M G, COOPER R M G, FARROW J B, PARKINSON G M. Defining the Paragoethite process for iron removal in zinc hydrometallurgy [J]. Hydrometallurgy, 2006, 81(2):104−129.

[13] ACHARYA S, ANAND S, DAS R P. Iron rejection through jarosite precipitation during acid pressure leaching of zinc leach residue [J]. Hydrometallurgy, 1992, 31(31): 101−110.

[14] DUTRIZAC J E. An overview of iron precipitation in hydrometallurgy [J]. Crystallization & Precipitation, 1987, 80(903): 259−283.

[15] MATTHES J, WAIBEL P, KELLER H B. A new infrared camera-based technology for the optimization of the Waelz process for zinc recycling [J]. Minerals Engineering, 2011, 24(8): 944−949.

[16] LUCHEVA B, ILIEV P, DRAGANOVA K, STEFANOVA V. Recovery of copper and silver from Waelz clinker wasted from zinc production [J]. Journal of Chemical Technology & Metallurgy, 2014, 49(1): 12−15.
[17] VERSCHEURE K, CAMP M V. Continuous fuming of zinc-bearing residues: Part II. the submerged-plasma zinc-fuming process [J]. Metallurgical and Materials Transactions B, 2007, 38(1): 21−33.
[18] HOANG J, REUTER M A, MATUSEWICZ R, HUGHES S, PIRET N. Top submerged lance direct zinc smelting [J]. Minerals Engineering, 2009, 22(9−10): 742−751.
[19] KIM B S, JEONG S B, LEE J C, SHIN D, MOON N I. Behaviors of lead and zinc in top submerged lance (TSL) plant at sukpo zinc refinery [J]. Materials Transactions, 2012, 53(5): 985−990.
[20] MANDIN D, SLOOT H A V D, GERVAIS C, BARNA R, MEHU J. Valorization of lead−zinc primary smelters slags [J]. Studies in Environmental Science, 1997, 71(97): 617−630.
[21] WANG Fu-sheng, CHE Xin. Status and trend of comprehensive utilization of zinc slag [J]. Tianjin Chemical Industry, 2010, 24(3): 1−3. (in Chinese)
[22] HE Shi-chao. Comprehensive utilization of iron concentrate separated from kiln slag in zinc hydrometallurgy [D]. Changsha: Central South University, 2013. (in Chinese)
[23] HE Shi-chao, LIU Zhi-hong, LIU Zhi-yong, LI Yu-hu, LI Qi-hou. Thermodynamic analysis of leaching of iron concentrate separated from kiln slag in zinc hydrometallurgy [J]. The Chinese Journal of Nonferrous Metals, 2013, 23(12): 3430−3439. (in Chinese)
[24] DEAN J A. Lange's handbook of chemistry [M]. WEI J F, transl. Beijing: Science Press, 2003. (in Chinese)
[25] FARMER V C. The infrared spectra of minerals [M]. YING Yu-pu, et al, trasl. Beijing: Science Press, 1982: 428. (in Chinese)
[26] WEN Lu. The infrared spectroscopy of minerals [M]. Chongqing: Chongqing University Press, 1989: 190. (in Chinese)
[27] DIETZEL M. Dissolution of silicates and the stability of polysilicic acid [J]. Geochimica et Cosmochimica Acta, 2000, 64(19): 3275−3281.
[28] WANG Hong-jun, ZHANG Wen-hai, LIU Zhi-hong, LI Qi-hou, LI Yu-hu, LIU Zhi-yong, HE Shi-chao. Novel process for comprehensive utilization of iron concentrate recovered from zinc kiln slag [J]. The Chinese Journal of Nonferrous Metals, 2016, 26(3): 673−680. (in Chinese)
[29] LIU Zhi-hong, PAN Qing-lin, LIU Zhi-yong, LI Yu-hu, LI Qi-hou. Reactive behaviors between As(Ⅲ) and metallic iron in acidic aqueous solution [J]. The Chinese Journal of Nonferrous Metals, 2015, 25(10): 2945−2952. (in Chinese)

湿法炼锌窑渣铁精矿中有价组分浸出行为及其机理

王红军[1,2]，刘智勇[1]，刘志宏[1]，李玉虎[1]，李思唯[1]，张文海[1,2]，李启厚[1]

1. 中南大学 冶金与环境学院，长沙 410083；
2. 中国瑞林工程技术有限公司 冶金所，南昌 330031

摘　要：盐酸浸出−喷雾热分解法被认为是高效清洁回收湿法炼锌窑渣铁精矿中有价金属的新方法。系统研究了Ag、Pb、Cu、Fe、As、Zn、Si 等元素在浸出过程中的行为。结果表明：采用 6 mol/L HCl 溶液，在液固比 10:1、温度 60 °C、浸出 120 min 的条件下，Ag、Pb、Cu、Fe、As、Zn 的浸出率分别为 99.91%、99.25%、95.12%、90.15%、87.58%和 58.15%。浸出过程中硅达到饱和，从溶液中析出无定型 SiO_2，由于其对溶液中的金属离子产生吸附作用，从而对窑渣铁精矿中有价金属的浸出产生不利影响，所以控制 SiO_2 的析出对浸出过程至关重要。

关键词：窑渣；铁精矿；盐酸浸出；无定形 SiO_2

(Edited by Xiang-qun LI)